INSTITUTE OF PHYSICS PUBLISHING JOURNAL OF PHYSICS: CONDENSED MATTER

J. Phys.: Condens. Matter **17** (2005) 6057–6080 doi:10.1088/0953-8984/17/38/011

Landau–Lifshitz equations and relaxation of spin wave modes in the Heisenberg model with dipole–exchange interaction

L V Lutsev

Research Institute 'Ferrite-Domen', Chernigovskaya 8, Saint Petersburg, 196084, Russia

E-mail: lutsev@domen.ru

Received 28 February 2005, in final form 22 August 2005
Published 9 September 2005
Online at stacks.iop.org/JPhysCM/17/6057

Abstract

Landau–Lifshitz equations and spin wave damping are derived from first principles by the spin operator diagram technique for the Heisenberg model with magnetic dipole and exchange interactions. It is found that spin excitations, which are determined by poles of effective Green functions, are given by solutions of the linearized pseudodifferential Landau–Lifshitz equations and the equation for the magnetostatic potential. For a normal magnetized ferromagnetic film the spin wave damping has been calculated in the one-loop approximation for a diagram expansion of the Green functions at low temperature. In the framework of the Heisenberg model the magnetic dipole interaction makes a major contribution to the long-wavelength spin wave relaxation in comparison with the exchange interaction. It is found that the damping decreases with increasing film thickness and applied magnetic field and increases directly proportionally to the temperature. For modes of high orders the damping is higher than for the first spin wave mode.

1. Introduction

Spin dynamics in ultrathin magnetic structures is of great interest due to the wide variety of industrial applications—magnetic memory cells, new tunnelling microscopy based on the time-resolved Kerr effect, microwave and optical signal processing. Spin waves in ultrathin ferromagnetic films and magnetic nanostructures are influenced by geometric confinement and atomic structures. This influence and the competition between the magnetic dipole interaction (MDI) and the exchange interaction can lead to unique spin excitations. An investigation of these excitations—localized spin wave modes in nanosized magnetic dots [1], wires [2] and inhomogeneously magnetized stripes [3], the measurement of spin mode excitation and relaxation in films using scanning Kerr imaging [4]—is an essential step in achieving an understanding of the spin wave dynamics of low-dimensional structures. The important

application of spin waves is realized in spin wave devices—microwave filters, delay lines, signal-to-noise enhancers, and optical signal processors [5, 6]. In order to design new nanosized spin wave devices based on ultrathin films, it is necessary to determine the spectra and damping of spin excitations in low-dimensional structures. This leads us to develop the Heisenberg model with magnetic dipole and exchange interactions (or, shortly, the dipole–exchange interaction). We consider the relaxation of spin excitations in the framework of this model and generalize the Landau–Lifshitz equations.

Pure ferromagnetic films with low spin wave damping are used in spin wave devices. In pure ferromagnetics—yttrium iron garnet $Y_3Fe_5O_{12}$ (YIG) [7–11], lithium ferrospinel $Li_{0.5}Fe_{2.5}O_4$ [12], $CdCr_2Se_4$ and EuO [8, 13, 14]—the spin wave damping is determined by intrinsic relaxation processes. At low temperatures the relaxation is induced by the MDI and occurs through the confluence of two magnons and through the splitting of a magnon into two magnons [8, 9, 11, 15–17]. In [11, 15–17] the spin wave damping is calculated for infinite or semi-infinite ferromagnets. But the fundamental problem of the magnetic relaxation in the Heisenberg model with magnetic dipole and exchange interactions for finite ferromagnetic samples has not yet been investigated comprehensively. The cause of this problem is the long-range action of the MDI. Due to the long-range character, the relatively weak MDI transforms the spin wave spectrum to the spectrum of the discrete mode type. The spin wave relaxation and the spin wave dynamics become dependent on the dimensions and shapes of ferromagnetic samples. On account of this, the Heisenberg model with magnetic dipole and exchange interactions for finite samples is essentially different from the Heisenberg model with only exchange interaction. In order to analyse the Heisenberg model with the dipole–exchange interaction we use the spin operator diagram technique [18–20]. Advantages of the spin operator diagram technique are: the uniform description of magneto-ordered systems in a large temperature range, the opportunity to calculate the spin wave damping at high temperatures, and more exact relationships describing spin wave scattering in comparison with other methods, which are based on diagram techniques for creation and annihilation magnon Bose operators [8, 21–23].

In this study, in section 3 we introduce the matrix of effective propagators and interactions (the $\mathcal{P}$-matrix), and the diagram expansion is expressed in terms of the two-site effective Green functions (effective propagators) and effective interaction lines. Spin excitations are determined by poles of the $\mathcal{P}$-matrix. In section 4, we show that in the framework of the Heisenberg model with the dipole–exchange interaction the calculation of the poles is equivalent to finding the simultaneous solution of the linearized pseudodifferential Landau–Lifshitz equations and the equation for the magnetostatic potential. Eigenvalues of the equation for the magnetostatic potential give the spin wave mode spectrum, which is dependent on the dimensions and shapes of ferromagnetic samples. We consider the Heisenberg model for the case of a normal magnetized ferromagnetic film and calculate the $\mathcal{P}$-matrix in the low-temperature approximation. The scattering on thermal excited spin wave modes, which interact with each other through the MDI, gives a major contribution to the relaxation of long-wavelength spin waves. In section 5 we calculate this contribution, which is determined by diagrams in the one-loop approximation and corresponds to the confluence of two magnons. The exchange interaction gives non-trivial terms in the damping in the two-loop approximation and these terms are small in comparison with the damping determined by the MDI. We have found that the damping, which is caused by the MDI, decreases with increasing film thickness and applied magnetic field and increases directly proportionally to the temperature. For modes with high mode numbers the spin wave damping is higher than for the first spin wave mode. For thin ferromagnetic films relaxation peaks appear. With increasing film thickness, these peaks are smoothed.

2. Spin operator diagram technique

Let us consider the Heisenberg model on a crystal lattice with the Hamiltonian

$$\mathcal{H} = -g\mu_B H \sum_{\vec{1}} S^z(\vec{1}) - \tfrac{1}{2} \sum_{\vec{1},\vec{1}'} J_{\mu\nu}(\vec{1}-\vec{1}') S^\mu(\vec{1}) S^\nu(\vec{1}'), \tag{1}$$

where H ($\vec{H} \parallel Oz$) is the external magnetic field; $\mu, \nu = -, +, z$. It is supposed that the summation in (1) and in the all following relations is performed over all repeating indices μ, ν. $\vec{1} \equiv \vec{r}_1, \vec{1}' \equiv \vec{r}_1{}'$ is the abridged notation of crystal lattice sites. The summation is carried out over the crystal lattice sites $\vec{1}, \vec{1}'$ in the volume V of the ferromagnetic sample. g and μ_B are the Landé factor and the Bohr magneton, respectively. $S^\mu(\vec{1})$ are the spin operators. $J_{\mu\nu}(\vec{1}-\vec{1}') = J_{\nu\mu}(\vec{1}'-\vec{1})$ is the interaction between spins, which is the sum of the exchange interaction $I_{\mu\nu}$ and the MDI

$$J_{\mu\nu}(\vec{1}-\vec{1}') = I_{\mu\nu}(\vec{1}-\vec{1}') - 4\pi(g\mu_B)^2 \nabla_\mu \Phi(\vec{r}-\vec{r}') \nabla'_\nu\big|_{\vec{r}=\vec{1},\vec{r}'=\vec{1}'}, \tag{2}$$

where $\Phi(\vec{r}-\vec{r}')$ is determined by the equation

$$\Delta\Phi(\vec{r}-\vec{r}') = \delta(\vec{r}-\vec{r}'),$$
$$\nabla_\mu = \{\nabla_-, \nabla_+, \nabla_z\} = \left\{ \frac{1}{2}\left(\frac{\partial}{\partial x} + \mathrm{i}\frac{\partial}{\partial y}\right), \frac{1}{2}\left(\frac{\partial}{\partial x} - \mathrm{i}\frac{\partial}{\partial y}\right), \frac{\partial}{\partial z} \right\}.$$

Spin excitations in the canonical spin ensemble, described by the Hamiltonian $\mathcal{H}$, are determined by the two-site temperature Green functions [18–20, 24, 25]

$$G^{(c)}_{\mu\nu}(\vec{1}, \vec{1}', \tau_1 - \tau_1') = \left\langle\!\left\langle \mathbf{T}\hat{S}^\mu(\vec{1}, \tau_1)\hat{S}^\nu(\vec{1}', \tau_1') \right\rangle\!\right\rangle,$$

where $\hat{S}^\alpha(\vec{n}, \tau) = \exp(\tau\mathcal{H}) S^\alpha(\vec{n}) \exp(-\tau\mathcal{H})$ are the spin operators in the Euclidean Heisenberg representation, $\tau \in [0, \beta]$, $\beta = 1/kT$, k is the Boltzmann constant, and T is the temperature. $\mathbf{T}$ is the τ-time ordering operator. $\langle\langle \cdots \rangle\rangle$ denotes averaging of spin operators calculated with $\exp(-\beta\mathcal{H})/\mathrm{Sp}\exp(-\beta\mathcal{H})$. The symbol Sp denotes the trace.

The Fourier transforms are defined in terms of the Matsubara frequencies $\omega_m = 2\pi m/\hbar\beta$ (m is an integer)

$$G^{(c)}_{\mu\nu}(\vec{1}, \vec{1}', \omega_m) = \int_0^\beta G^{(c)}_{\mu\nu}(\vec{1}, \vec{1}', \tau) \exp(-\mathrm{i}\hbar\omega_m\tau)\, \mathrm{d}\tau. \tag{3}$$

The Green functions $G^{(c)}_{\mu\nu}(\vec{1}, \vec{1}', \omega_m)$ can be expanded with respect to the interaction $J_{\mu\nu}(\vec{1}-\vec{1}')$ [18–20]. Each term of this expansion $\sum_{n=0} Q^{(n)}_{\mu\nu}$ is represented by a diagram constructed of propagators, vertices, blocks and interaction lines.

1. Propagators. Spin propagators

$$D_\pm(\vec{1}, \vec{1}', \omega_m) = \frac{\delta_{\vec{1},\vec{1}'}}{p_0 \pm \mathrm{i}\beta\hbar\omega_m}, \tag{4}$$

where $p_0 = \beta g\mu_B H$, are determined for the spin ensemble without any interaction between spins. The propagators $D_\pm(\vec{1}, \vec{1}', \omega_m)$ are represented by directed lines in diagrams (figure 1(a)). The directions of the arrows show the direction of growth of the frequency variable ω_m.

2. Vertices. There are five types of vertices (figure 1(b)). Vertices a, b are the start and end points of propagators, respectively. In analytical expressions of diagrams the vertex a corresponds with the factor 2 and the vertex b with the factor 1. The vertex c ties three propagators and corresponds with the factor (-1) in analytical expressions. The vertex d with

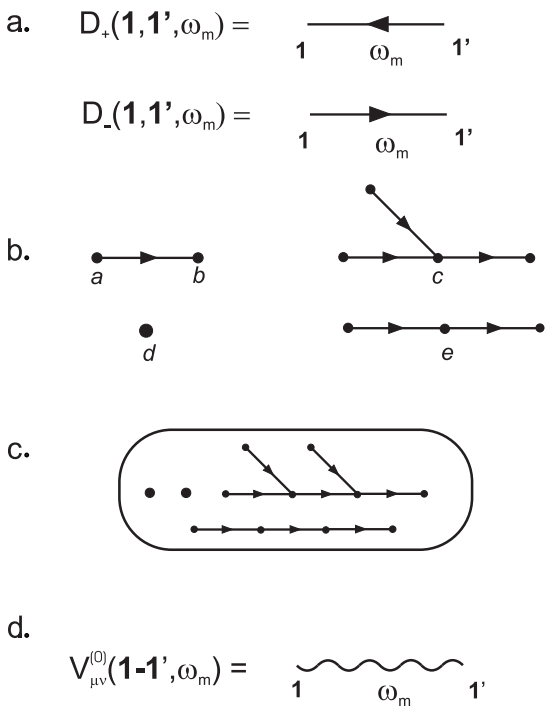

Figure 1. (a) Propagators $D_{\pm}$, (b) vertices, (c) block with four isolated parts and (d) interaction lines $V^{(0)}_{\mu\nu}$.

the factor 1 is defined as a single vertex. The vertex e ties two propagators. The factor of the e-vertex is equal to (-1).

3. Blocks. Blocks contain propagators and isolated vertices d (figure 1(c)). Propagators can be connected through vertices c, e. In analytical expressions of the diagram expansion each block corresponds with the block factor $B^{[\kappa-1]}(p_0)$, where κ is the number of isolated parts in the block. The factor $B^{[\kappa-1]}(p_0)$ is expressed by partial derivatives of the Brillouin function B_S for the spin S with respect to p_0

$$B(p_0) = \langle\langle S^z\rangle\rangle_0 = SB_S(Sp_0)$$
$$B^{[n]}(p_0) = S\frac{\partial^n B_S(Sp_0)}{\partial p_0^n}, \tag{5}$$

where $\langle\langle\cdots\rangle\rangle_0$ denotes the statistical averaging performed over the states described by the Hamiltonian $\mathcal{H}$ (1) without the interaction $J_{\mu\nu}$ between spins. $B_S(x) = (1 + 1/2S)\coth[(1 + 1/2S)x] - (1/2S)\coth(x/2S)$.

4. Interaction lines. The interaction line $V^{(0)}_{\mu\nu}(\vec{1}-\vec{1}', \omega_m) = \beta J_{\mu\nu}(\vec{1}-\vec{1}')$ connects two vertices in a diagram (figure 1(d)). The correspondence between the first index μ of the interaction line $V^{(0)}_{\mu\nu}$ and the vertex type is the following. 1: If $\mu = -$, then the left end point of $V^{(0)}_{-\nu}$ is bound to the vertex a; 2: if $\mu = +$, then this end point is bound to the vertices b or c; 3: if $\mu = z$, then the end is bound to the vertices d or e. The analogous correspondence is satisfied for the right end ν of $V^{(0)}_{\mu\nu}$.

The general form of the analytical expression of the diagram $Q^{(n)}_{\mu\ldots\nu}$ is written as [18–20]

$$Q^{(n)}_{\mu\ldots\nu}(\vec{1}^o,\ldots,\vec{k}^o,\omega^o_{m_1},\ldots,\omega^o_{m_k}) = (-1)^L 2^{m_a}\frac{P_n}{2^n n!}\prod_l B^{[\kappa_l-1]}(p_0)\prod_{\vec{i},\vec{j}\in l}^{\kappa_l}\delta_{\vec{i},\vec{j}}$$
$$\times \sum_{\substack{\vec{1},\ldots\vec{n}\\ \vec{1}'\ldots\vec{n}'}}\sum_{m_i} V^{(0)}_{\alpha\gamma}(\vec{1}-\vec{1}',\omega_{m_1})\times\cdots\times V^{(0)}_{\rho\sigma}(\vec{n}-\vec{n}',\omega_{m_n})$$
$$\times \prod_{\vec{s},\vec{s}'}^{I_D} D_-(\vec{s},\vec{s}',\omega_{m_s})\prod_v^{I_v}\delta\left(\sum_{r\in v}\beta\hbar\omega_{m_r}\right), \tag{6}$$

where $\vec{1}^o,\ldots,\vec{k}^o,\omega^o_{m_1},\ldots,\omega^o_{m_k}$ are the external lattice and frequency variables. m_a is the number of a-vertices in a diagram. L is the number of c- and e-vertices. P_n is the number of topological equivalent diagrams. $2n$ is the number of vertices connected with n interaction lines $V^{(0)}_{\alpha\gamma}\ldots V^{(0)}_{\rho\sigma}$. The product $\prod_l$ is performed over all blocks of a diagram. κ_l is the number of isolated parts in block l. The term $\prod_{\vec{i},\vec{j}\in l}^{\kappa_l}\delta_{\vec{i},\vec{j}}$ denotes that all isolated parts in block l are determined on a single-crystal lattice site. I_D is the number of propagators in a diagram. I_v is the number of vertices in a diagram. $\sum_{m_i}$ denotes the summation performed over all inner frequency variables. The term $\prod_v^{I_v}\delta\left(\sum_{r\in v}\beta\hbar\omega_{m_r}\right)$ gives the frequency conservation in each vertex v, i.e. the sum of frequencies of propagators and interaction lines, which come in and go out from the vertex v, is equal to 0. The vertex d can be connected with the single interaction line. In the analytical expression this corresponds to the factor $\delta(\beta\hbar\omega_m)$.

The lattice variables $\vec{s},\vec{s}'$ of propagators D_- can be inner or external. In the first case, end points of propagators are connected with the end points $\{\vec{1},\vec{1}',\ldots,\vec{n},\vec{n}'\}$ of interaction lines $V^{(0)}_{\alpha\gamma}\ldots V^{(0)}_{\rho\sigma}$ and the summation $\sum_{\substack{\vec{1},\ldots\vec{n}\\ \vec{1}'\ldots\vec{n}'}}\sum_{m_i}$ is performed. In the second case, end points of propagators are not connected with interaction lines.

3. Self-consistent-field approximation, effective propagators and effective interaction lines

3.1. Self-consistent field

The self-consistent-field approximation is equivalent to a rearrangement of the terms in the Hamiltonian $\mathcal{H}$. The exchange and dipole magnetic fields are added to the applied magnetic field $\vec{H}$

$$H^{(\mathrm{ex})}_\mu(\vec{1}) = (g\mu_\mathrm{B})^{-1}\sum_{\vec{1}'} I_{\mu\nu}(\vec{1}-\vec{1}')\langle\langle S^\nu(\vec{1}')\rangle\rangle$$
$$H^{(m)}_\mu(\vec{1}) = -4\pi g\mu_\mathrm{B}\nabla_\mu\sum_{\vec{1}'}\Phi(\vec{r}-\vec{r}')\nabla'_\nu\langle\langle S^\nu(\vec{r}')\rangle\rangle\Big|_{\substack{\vec{r}=\vec{1}\\ \vec{r}'=\vec{1}'}}, \tag{7}$$

where $\langle\langle S^\nu(\vec{r})\rangle\rangle = \langle\langle S^z(\vec{r})\rangle\rangle\delta_{\nu z}$ is the statistical average spin. The dipole magnetic field can be written as

$$H^{(m)}_\mu(\vec{1}) = \nabla_\mu\int_V\frac{1}{|\vec{r}-\vec{r}'|}\nabla'_\nu M^\nu(\vec{r}')\,\mathrm{d}^3r'\Big|_{\vec{r}=\vec{1}} + H^{(a)}_\mu(\vec{1}),$$

where the first term is the depolarizing magnetic field of the continuum ferromagnetic sample; $M^\nu(\vec{r}) = g\mu_\mathrm{B}\langle\langle S^\nu(\vec{r})\rangle\rangle/V_a$ is the vector of the magnetic moment density, which is defined by the averaging over the atomic volume V_a;

$$H^{(a)}_\mu(\vec{1}) = V_a\nabla_\mu\sum_{\vec{1}'}\frac{1}{|\vec{r}-\vec{r}'|}\nabla'_\nu M^\nu(\vec{r}') - \nabla_\mu\int_V\frac{1}{|\vec{r}-\vec{r}''|}\nabla''_\nu M^\nu(\vec{r}'')\,\mathrm{d}^3r''\Big|_{\substack{\vec{r}=\vec{1}\\ \vec{r}'=\vec{1}'}}$$

is the anisotropy magnetic field, which depends on the type of the lattice and the sample size. If the lattice is of the cubic type and the sample size is much greater than the lattice constant a, then $H_\mu^{(a)}(\vec{1}) = 0$ [7]. In other cases, $H_\mu^{(a)}(\vec{1}) \neq 0$ and size- and lattice-dependent effects must be taken into account [26, 27].

In the framework of the diagram technique the rearrangement in the Hamiltonian $\mathcal{H}$ corresponds to the summation of all diagrams that can be divided into two parts through breaking an interaction line. One of the parts does not have external vertices (so-called one-tail part of the diagrams) [18–20]. The summation of one-tail parts gives the summary field $\vec{H}^{(c)} = \vec{H} + \vec{H}^{(\mathrm{ex})} + \vec{H}^{(m)}$. The magnetic field $H_\mu^{(m)}(\vec{r})$ depends on the shape of the ferromagnetic sample. If the sample has ellipsoidal shape, the lattice is of the cubic type and the sample size is much greater than a, then the field $H_\mu^{(m)}(\vec{r})$ is uniform [28]. If the summary field $\vec{H}^{(c)}$ is not directed along the axis Oz, then we choose the basis (x', y', z') such that $\vec{H}^{(c)} \parallel Oz'$. From the equilibrium condition $[\vec{H}^{(c)} \times \langle\langle \vec{S} \rangle\rangle] = 0$ it follows that $\langle\langle \vec{S} \rangle\rangle \parallel \vec{H}^{(c)} \parallel Oz'$. After transformation to spin operators S^ν in coordinates (x', y', z') the diagram expansion is given by relation (6), where the substitution $p_0 \to p = \beta g \mu_\mathrm{B} H_z^{(c)}$ in the propagator D_- in relation (4) is performed. After this transformation all one-tail parts of diagrams are not taken into account. In sections 4, 5 we will consider the case of a normal magnetized ferromagnetic film with a cubic lattice and with thickness greater than a. We suppose that $\vec{H}, \vec{H}^{(\mathrm{ex})}, \vec{H}^{(m)} \parallel Oz$. In this case, for normal magnetized films the depolarizing magnetic field $\vec{H}^{(m)}$ is equal to $-4\pi\vec{M}$ [28].

3.2. Spin excitations and $\mathcal{P}$-matrix

The next approximation is the approximation of effective propagators and effective interactions. In the framework of this approximation we determine spin excitations and introduce the matrix of effective propagators and effective interactions $\mathcal{P} = \|P_{AB}(\vec{1}, \vec{1}', \omega_m)\|$. We compose the $\mathcal{P}$-matrix from analytical expressions of connected diagrams with two external sites. These sites are end points of propagators, single vertices d, or end points of interaction lines. Accordingly, multiindices $A = (a\mu)$, $B = (b\nu)$ are the double indices, where $\mu, \nu = \{-, +, z\}$ and indices a, b point out that A, B belong to a propagator or to a d-vertex ($a, b = 1$), or belong to an interaction line ($a, b = 2$). The zero-order approximation $\mathcal{P}^{(0)}$ of the $\mathcal{P}$-matrix is determined by the matrix of the bare interaction $\mathcal{V}^{(0)} = \|V_{\mu\nu}^{(0)}(\vec{1}, \vec{1}', \omega_m)\|$ and by the two-site Green functions (3) in the self-consistent-field approximation $\mathcal{G}^{(0)} = \|G_{\mu\nu}^{(0)}\|$, given on a crystal lattice site

$$\mathcal{P}^{(0)} = \begin{pmatrix} \|P^{(0)}_{(1\mu)(1\nu)}\| & \vdots & \|P^{(0)}_{(1\mu)(2\nu)}\| \\ \cdots & \cdots & \cdots \\ \|P^{(0)}_{(2\mu)(1\nu)}\| & \vdots & \|P^{(0)}_{(2\mu)(2\nu)}\| \end{pmatrix} = \begin{pmatrix} \|G^{(0)}_{\mu\nu}\| & \vdots & 0 \\ \cdots & \cdots & \cdots \\ 0 & \vdots & \|V^{(0)}_{\mu\nu}\| \end{pmatrix},$$

where

$$\|G_{\mu\nu}^{(0)}\| = \begin{pmatrix} 0 & G_{-+}^{(0)} & 0 \\ G_{+-}^{(0)} & 0 & 0 \\ 0 & 0 & G_{zz}^{(0)} \end{pmatrix} = \begin{pmatrix} 0 & 2B(p)D_-(\vec{1}, \vec{1}', \omega_m) & 0 \\ 2B(p)D_+(\vec{1}, \vec{1}', \omega_m) & 0 & 0 \\ 0 & 0 & B^{[1]}(p)\delta_{\vec{1}\vec{1}'}\delta_{m0} \end{pmatrix} \tag{8}$$

with the propagator (4), in which the substitution $p_0 \to p$ is performed:

$$D_\pm(\vec{1}, \vec{1}', \omega_m) = \frac{\delta_{\vec{1},\vec{1}'}}{p \pm \mathrm{i}\beta\hbar\omega_m}.$$

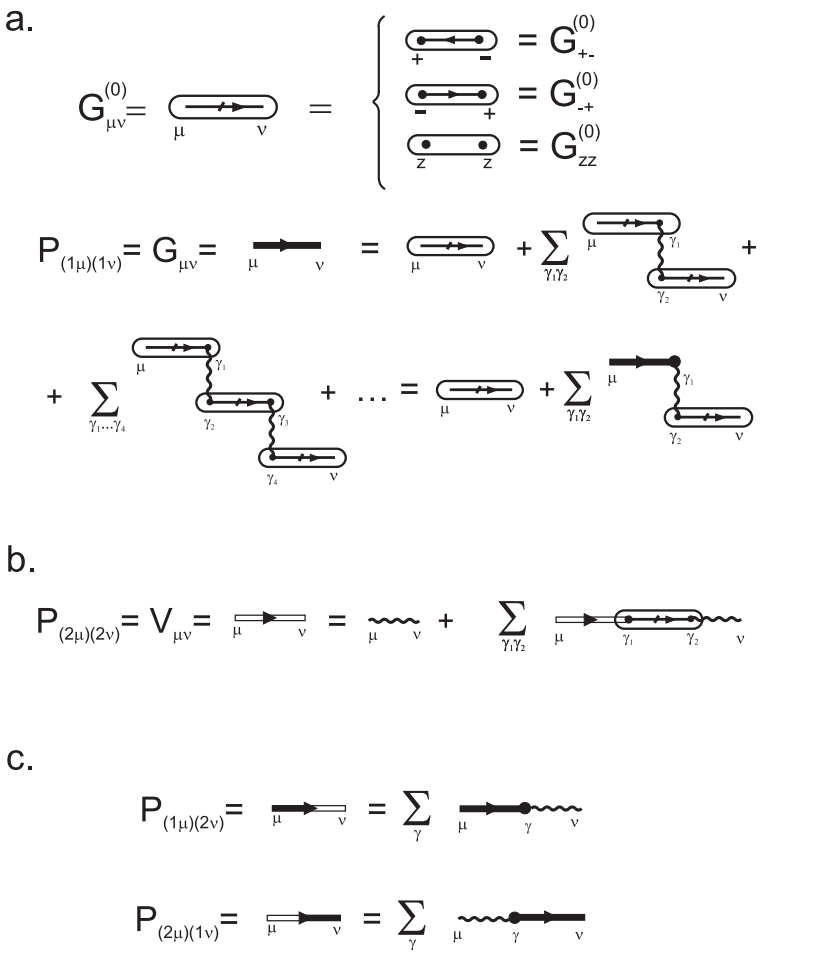

Figure 2. (a) Definition of effective propagators $P_{(1\mu)(1\nu)} = G_{\mu\nu}$ via the bare two-site Green functions $G^{(0)}_{\mu\nu}$. (b) Definition of effective interaction lines $P_{(2\mu)(2\nu)} = V_{\mu\nu}$. (c) Definition of intersecting terms $P_{(1\mu)(2\nu)}$, $P_{(2\mu)(1\nu)}$.

The $\mathcal{P}$-matrix is obtained by means of the summation of the $\mathcal{P}^{(0)}$-matrix—the summation of all diagram chains consisting of the bare Green functions $G^{(0)}_{\mu\nu}$ and the bare interaction lines $V^{(0)}_{\mu\nu}$ (figure 2). These chains of propagators and interaction lines do not have any loop insertion. Analytical expressions of the considered diagrams can be written in accordance with relation (6). The summation gives an equation of the Dyson type, which forms the relationship between $\mathcal{P}^{(0)}$- and $\mathcal{P}$-matrices

$$\mathcal{P} = \mathcal{P}^{(0)} + \mathcal{P}\sigma\mathcal{P}^{(0)}, \tag{9}$$

where

$$\sigma = \begin{pmatrix} 0 & \vdots & \mathcal{E} \\ \cdots & \cdots & \cdots \\ \mathcal{E} & \vdots & 0 \end{pmatrix}, \qquad \mathcal{E} = \|\delta_{\mu\nu}\| \text{ is the diagonal matrix.}$$

Taking into account $\mathcal{E} - \mathcal{G}^{(0)}\mathcal{V}^{(0)} = \mathcal{G}^{(0)}(\mathcal{E} - \mathcal{V}^{(0)}\mathcal{G}^{(0)})\mathcal{G}^{(0)-1}$, we find that the solution of equation (9) is the matrix

$$\mathcal{P} = \mathcal{P}^{(0)}(1 - \sigma\mathcal{P}^{(0)})^{-1} = \begin{pmatrix} \mathcal{G}^{(0)}(\mathcal{E} - \mathcal{V}^{(0)}\mathcal{G}^{(0)})^{-1} & \vdots & (\mathcal{E} - \mathcal{G}^{(0)}\mathcal{V}^{(0)})^{-1}\mathcal{G}^{(0)}\mathcal{V}^{(0)} \\ \cdots & \cdots & \cdots \\ \mathcal{V}^{(0)}\mathcal{G}^{(0)}(\mathcal{E} - \mathcal{V}^{(0)}\mathcal{G}^{(0)})^{-1} & \vdots & \mathcal{V}^{(0)}(\mathcal{E} - \mathcal{G}^{(0)}\mathcal{V}^{(0)})^{-1} \end{pmatrix}. \tag{10}$$

The $\mathcal{P}$-matrix consists of effective propagators (two-site effective Green functions) $\mathcal{G} = \|G_{\mu\nu}\| = \mathcal{G}^{(0)}(\mathcal{E} - \mathcal{V}^{(0)}\mathcal{G}^{(0)})^{-1}$, where $G_{\mu\nu} = P_{(1\mu)(1\nu)}$, effective interactions $\mathcal{V} = \|V_{\mu\nu}\| = \mathcal{V}^{(0)}(\mathcal{E} - \mathcal{G}^{(0)}\mathcal{V}^{(0)})^{-1}$, where $V_{\mu\nu} = P_{(2\mu)(2\nu)}$, and intersecting terms $P_{(1\mu)(2\nu)}$, $P_{(2\mu)(1\nu)}$ (figure 2). Effective propagators, effective interactions and intersecting terms are denoted in diagrams by directed thick lines, empty lines and compositions of the thick line–empty line, respectively. The $\mathcal{P}$-matrix determines the spectrum of quasi-particle excitations in the spin ensemble. Spectrum relations for spin excitations are given by the $\mathcal{P}$-matrix poles—by zero eigenvalues of the operator $1 - \sigma\mathcal{P}^{(0)}$ or, equivalently, by $\mathcal{E} - \mathcal{V}^{(0)}\mathcal{G}^{(0)}$ under the analytical continuation

$$\begin{aligned} &\mathrm{i}\omega_m \to \omega + \mathrm{i}\varepsilon\,\mathrm{sgn}\,\omega \\ &\delta(\beta\hbar\omega_m) = \delta_{m0} \to \frac{1}{\beta\hbar(\omega + \mathrm{i}\varepsilon\,\mathrm{sgn}\,\omega)} \qquad (\varepsilon \to +0). \end{aligned} \tag{11}$$

Spectral parameters λ, which can be discrete or continuous, are in correspondence with vector eigenfunctions $|\lambda\rangle \equiv \|h_\mu^{(\lambda)}(\vec{1}, \omega_m)\|$

$$(\mathcal{E} - \mathcal{V}^{(0)}\mathcal{G}^{(0)})\|h_\mu^{(\lambda)}(\vec{1}, \omega_m)\| = 0. \tag{12}$$

The decomposition of the $\mathcal{P}$-matrix (10) over the basis of eigenfunctions $|\lambda\rangle$ determines the effective spin propagators and effective interactions in the quasi-particle λ-representation. The elements of the $\mathcal{P}$-matrix in the λ-representation have the form

$$\begin{aligned} P_{A_iA_j}(\lambda_i, \lambda_j, \omega_m) &= \langle\lambda_i|P_{(a_i\mu_i)(a_j\mu_j)}(\omega_m)|\lambda_j\rangle \\ &= \sum_{\vec{1},\vec{1}'} h_{\mu_i}^{(\lambda_i)*}(\vec{1}, \omega_m)P_{(a_i\mu_i)(a_j\mu_j)}(\vec{1}, \vec{1}', \omega_m)h_{\mu_j}^{(\lambda_j)}(\vec{1}', \omega_m), \end{aligned} \tag{13}$$

where $A_{i(j)} = (a_{i(j)}\mu_{i(j)})$.

3.3. Diagram technique with effective propagators and interaction lines

Introduction of the $\mathcal{P}$-matrix allows us to perform a partial summation and to substitute effective propagators and effective interaction lines for bare propagators and interactions in the diagram expansion (figure 3). Substituting effective G_{-+}-propagators and $\mathcal{P}$-matrix elements for bare propagators and bare interaction lines in the diagram expansion (6), we obtain analytical expressions of diagrams, which do not contain bare propagators. We say that these diagrams are *Eff*-diagrams. The general form of the analytical expression of the *Eff*-diagram in the λ-representation is

$$\begin{aligned} Q_{\mu\ldots\nu}^{(n,\mathrm{eff})}(\vec{1}^o, \ldots, \vec{k}^o, \omega_{m_1}^o, \ldots, \omega_{m_k}^o) &= (-1)^L 2^{m'_a}\frac{P_n}{2^n n!}\prod_l \xi^{(l)} \sum_{m_i} \sum_{\substack{\lambda_1\ldots\lambda_{2n} \\ A_1\ldots A_{2n}}} P_{A_1A_2}(\lambda_1, \lambda_2, \omega_{m_1}) \\ &\times \cdots \times P_{A_{2n-1}A_{2n}}(\lambda_{2n-1}, \lambda_{2n}, \omega_{m_n}) \prod_{s,s'}^{I_G} G_{-+}(\lambda_s, \lambda_{s'}, \omega_{m_s}) \\ &\times \prod_{\bar{l}} N_{\mu_{j_1}\ldots\mu_{j_\zeta}}^{(\bar{l})}(\lambda_{j_1}, \ldots, \lambda_{j_\zeta}, \omega_{m_1}, \ldots, \omega_{m_\zeta}) \prod_v^{I_v} \delta\left(\sum_{r\in v} \beta\hbar\omega_{m_r}\right), \end{aligned} \tag{14}$$

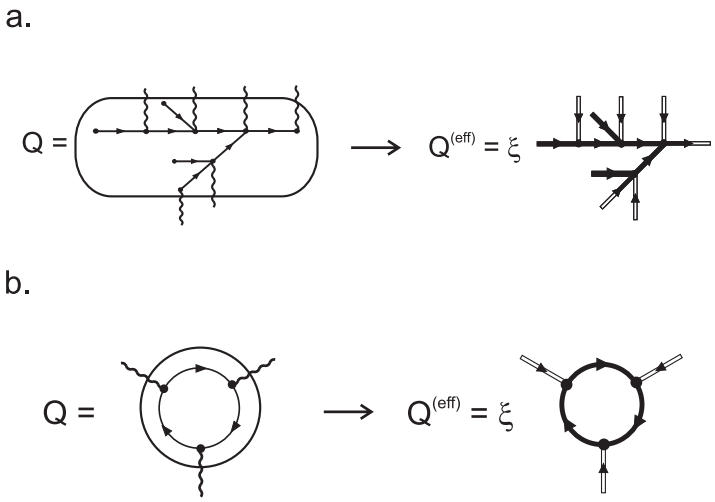

Figure 3. Partial summation and substitution effective propagators and effective interaction lines for bare propagators and interactions in diagrams. (a) Decomposition of the block without isolated parts under performing the transformation from bare propagators and interaction lines to effective ones. (b) Bare diagram Q with the propagator loop and the *Eff*-diagram $Q^{(\mathrm{eff})}$ corresponding to Q. ξ is the factor which arises from the decomposition of bare diagram blocks.

where $n\mathcal{P}$-matrix terms $P_{A_i A_{i+1}}$ are intersecting terms or effective interactions, i.e. at least one of the double indices A_i or A_{i+1} of the $\mathcal{P}$-matrix term has the form $A = (2\mu_j)$. $G_{-+}(\lambda_s, \lambda_{s'}, \omega_{m_s}) = P_{(1-)(1+)}(\lambda_s, \lambda_{s'}, \omega_{m_s})$. m'_a is the number of external vertices a. I_v is the number of vertices in the *Eff*-diagram. I_G is the number of G_{-+}-propagators. The product $\xi = \prod_l \xi^{(l)}$ is performed over all blocks l of the bare diagram. The factor $\xi^{(l)}$ arises from the decomposition of block l of the bare diagram (figure 3). For a block without isolated parts in the bare diagram the factor $\xi^{(l)}$ is written in the form

$$\xi^{(l)} = 2^{m''_a - u_D} B(p)^{1-u_c-u_D},$$

where m''_a is the number of inner (connected with interaction lines) a-vertices in block l; u_D is the number of D_--propagators; u_c is the number of propagator loops in block l. $\sum_{m_i}$ denotes the summation performed over all inner frequency variables. $N^{(\bar{l})}_{\mu_{j_1}\ldots\mu_{j_\zeta}}(\lambda_{j_1}, \ldots, \lambda_{j_\zeta}, \omega_{m_1}, \ldots, \omega_{m_\zeta}) = \sum_{\vec{1}} h^{(\lambda_{j_1})}_{\mu_{j_1}}(\vec{1}, \omega_{m_1}) \ldots h^{(\lambda_{j_\zeta})}_{\mu_{j_\zeta}}(\vec{1}, \omega_{m_\zeta})$ is the block factor, which arises in the λ-representation due to the coincidence of crystal lattice sites for isolated parts contained in block $\bar{l}$. The factor $N^{(\bar{l})}$ determines the overlapping of quasi-particle eigenfunctions. The product $\prod_{\bar{l}} N^{(\bar{l})}$ is performed over all forming blocks $\bar{l}$ of the *Eff*-diagram. ζ is the number of lines, which come in or go out from block $\bar{l}$ of the *Eff*-diagram. The term $\prod_v^{I_v} \delta\left(\sum_{r\in v} \beta\hbar\omega_{m_r}\right)$ gives the frequency conservation in each vertex v.

4. Excitations in the Heisenberg model with dipole–exchange interaction

4.1. Derivation of dispersion equations in the general form

Now we find the effective propagators, effective interactions and dispersion relations for spin excitations in the Heisenberg model with dipole–exchange interaction given by relation (2): $\mathcal{V}^{(0)}(\vec{1}-\vec{1}', \omega_m) = \mathcal{V}^{(\mathrm{exch})}(\vec{1}-\vec{1}', \omega_m) + \mathcal{V}^{(\mathrm{dip})}(\vec{1}-\vec{1}', \omega_m)$, where $\mathcal{V}^{(\mathrm{exch})} = \|\beta I_{\mu\nu}(\vec{1}-\vec{1}')\|$ and

$\mathcal{V}^{(\mathrm{dip})} = \|-4\pi\beta(g\mu_\mathrm{B})^2\nabla_\mu\Phi(\vec{r}-\vec{r}')\nabla'_\nu\|_{\vec{r}=\vec{1},\vec{r}'=\vec{1}'}$. The equation, which determines the matrix $\mathcal{G}$ of effective propagators, is derived from equation (9) for the $\mathcal{P}$-matrix

$$\mathcal{G} = \mathcal{G}^{(0)} + \mathcal{G}(\mathcal{V}^{(\mathrm{exch})} + \mathcal{V}^{(\mathrm{dip})})\mathcal{G}^{(0)}, \tag{15}$$

where $\mathcal{G}^{(0)} = \|G^{(0)}_{\mu\nu}\|$ is the matrix of bare propagators (8).

The dispersion relations for spin excitations are determined by $\mathcal{P}$-matrix poles which coincide with poles of the matrix $\mathcal{G}$ of effective propagators given by equation (15). Accordingly, the dispersion relations can be derived from the eigenvalues of equation (12). Since the considered interaction is the sum of exchange and magnetic dipole interactions, we can obtain the eigenvalues and eigenfunctions of equation (12) by a two-step procedure. In the first stage, we perform the summation of diagrams, taking into account the exchange interaction, and find the propagator matrix $\mathcal{G}^{(1)} = \|G^{(1)}_{\mu\nu}\|$

$$\mathcal{G}^{(1)} = \mathcal{G}^{(0)} + \mathcal{G}^{(0)}\mathcal{V}^{(\mathrm{exch})}\mathcal{G}^{(1)}. \tag{16}$$

In the second stage, the summation of diagrams with dipole interaction lines is performed. This gives the equation for the matrix $\mathcal{G}$ of effective propagators expressed in terms of the matrix $\mathcal{G}^{(1)}$

$$\mathcal{G} = \mathcal{G}^{(1)} + \mathcal{G}\mathcal{V}^{(\mathrm{dip})}\mathcal{G}^{(1)}. \tag{17}$$

Thus, the solution of equation (15), which determines the matrix $\mathcal{G}$, is equivalent to the solution of equations (16), (17). After the performed two-step summation, equation (12) for eigenfunctions $h^{(\lambda)}_\mu$ is written in the more convenient form

$$h^{(\lambda)}_\mu(\vec{1},\omega_m) - \sum_{\substack{\rho,\sigma\\ \vec{1}'\vec{1}''}} V^{(\mathrm{dip})}_{\mu\rho}(\vec{1}-\vec{1}',\omega_m)G^{(1)}_{\rho\sigma}(\vec{1}',\vec{1}'',\omega_m)h^{(\lambda)}_\sigma(\vec{1}'',\omega_m) = 0. \tag{18}$$

The solution of simultaneous equations (16), (18) gives the dispersion relations for spin excitations. These equations can be reduced to linearized Landau–Lifshitz equations in the generalized form and the equation for the magnetostatic potential. In order to perform this transformation one needs to make a transition to the retarded Green functions.

4.2. *Linearized Landau–Lifshitz equations*

We transform matrix equation (16) to equations describing small variations of the magnetic moment density (or the variable magnetization), m_ν. The variable magnetization m_ν under the action of the magnetic field h_ν is given by the retarded Green functions, which are determined by the analytical continued values of the propagator matrix $\mathcal{G}^{(1)}$ [29]

$$m_\nu(\vec{1},\omega) = \frac{\beta(g\mu_\mathrm{B})^2}{V_a}\sum_{\rho,\vec{1}'} G^{(1)}_{\nu\rho}(\vec{1},\vec{1}',\omega_m)\Big|_{\mathrm{i}\omega_m\to\omega-\mathrm{i}\varepsilon} h_\rho(\vec{1}',\omega). \tag{19}$$

The analytical continuation $\mathrm{i}\omega_m \to \omega - \mathrm{i}\varepsilon$ defines the retarded Green functions. $h_\rho(\vec{1},\omega)$ is the field of the magnetic dipole–dipole interaction acting on spins. By multiplying matrix equation (16) by $\mathcal{G}^{(0)-1}$ from the left and by h_ρ from the right, performing the analytical continuation $\mathrm{i}\omega_m \to \omega - \mathrm{i}\varepsilon$ and taking into account relation (19), we get matrix equation (16) in the form of simultaneous equations

$$\sum_{\nu,\vec{1}'}[G^{(0)-1}_{\rho\nu}(\vec{1},\vec{1}',\omega) - \beta I_{\rho\nu}(\vec{1}-\vec{1}')]m_\nu(\vec{1}',\omega) = \frac{\beta(g\mu_\mathrm{B})^2}{V_a}h_\rho(\vec{1},\omega). \tag{20}$$

We suppose that the exchange interaction is isotropic, $2I_{-+} = 2I_{+-} = I_{zz} = I$, and the Fourier transform of the exchange interaction with respect to the lattice variables is

$\tilde{I}(\vec{k}) = \sum_{\vec{1}} I(\vec{1}) \exp(-\mathrm{i}\vec{k}\vec{1}) = \tilde{I}(0) - wk^2$. Then, after these suppositions equations (20) have the form

$$\hat{E}_{\pm} m_{\pm}(\vec{1}, \omega) = 2\gamma M(\vec{1}) h_{\mp}(\vec{1}, \omega) \tag{21}$$

$$\hat{E}_z m_z(\vec{1}, \omega) = \frac{B^{[1]}(p)}{B(p)} \gamma M(\vec{1}) h_z(\vec{1}, \omega), \tag{22}$$

where $\gamma = g\mu_{\mathrm{B}}/\hbar$ is the gyromagnetic ratio; $M(\vec{1}) = g\mu_{\mathrm{B}} B(p)/V_a$ is the magnetic moment density at the low-temperature approximation. We say that the operators $\hat{E}_{\pm}$, $\hat{E}_z$:

$$\hat{E}_{\pm} m_{\pm}(\vec{1}, \omega) = [\gamma(H(\vec{1}) + H^{(m)}(\vec{1})) \pm \omega] m_{\pm}(\vec{1}, \omega) + \frac{4\pi\gamma\alpha M(\vec{1})}{V_b} \sum_{\vec{1}'} \int_{V_b} k^2 \exp[\mathrm{i}\vec{k}(\vec{1} - \vec{1}')] m_{\pm}(\vec{1}', \omega)\, \mathrm{d}^3 k$$

$$\hat{E}_z m_z(\vec{1}, \omega) = \omega \left\{ m_z(\vec{1}, \omega) - \frac{\beta B^{[1]}(p)}{V_b} \sum_{\vec{1}'} \int_{V_b} \tilde{I}(\vec{k}) \exp[\mathrm{i}\vec{k}(\vec{1} - \vec{1}')] m_z(\vec{1}', \omega)\, \mathrm{d}^3 k \right\}$$

are Landau–Lifshitz operators. The field $H^{(m)}(\vec{1})$ is defined by relation (7) and depends on the magnetic moment density $M(\vec{1})$; $V_b = (2\pi)^3/V_a$ is the volume of the first Brillouin zone; $\alpha = wV_a/4\pi(g\mu_{\mathrm{B}})^2$ is the exchange interaction constant. If the scale of the spatial distribution of the variable magnetization $m_\nu(\vec{1}, \omega)$ and the sample size are much greater than the lattice constant a, then the sum over the lattice variables $\sum_{\vec{1}}$ in $\hat{E}_{\pm}$, $\hat{E}_z$ can be converted into an integral over the sample volume $V_a^{-1} \int \mathrm{d}^3 r$ and the operators $\hat{E}_{\pm}$, $\hat{E}_z$ are pseudodifferential operators of order 2 [30].

Equations (21), (22) have the generalized form of the Landau–Lifshitz equations [8, 9]. Solutions $m_{\pm}$ of equations (21) depend on temperature, because $\beta = 1/kT$ is contained in the variable of the Brillouin function $B(p)$, through which the magnetic moment density $M(\vec{1})$ is expressed. Equation (22) describes longitudinal variations of the variable magnetization under the influence of the field h_z. At low temperature the derivative of the Brillouin function $B^{[1]}(p)$ tends to 0 and the longitudinal variable magnetization m_z is negligible.

4.3. Equation for the magnetostatic potential and dispersion relations

From the form of the magnetic dipole interaction in relation (2) it follows that the field h_ν in equations (18), (19) is magnetostatic, i.e. it is expressed in terms of the magnetostatic potential φ: $h_\nu = -\nabla_\nu \varphi$. We transform equation (18) to the equation for the magnetostatic potential $\varphi(\vec{r}, \omega)$. Taking into account formula (19) and the explicit form of the magnetic dipole interaction in relation (2), performing the derivation ∇_μ, the analytical continuation $\mathrm{i}\omega_m \to \omega - \mathrm{i}\varepsilon$ and the summation of equation (18) over the index μ, we obtain the equation expressed in terms of φ, m_ν

$$-\Delta\varphi(\vec{r}, \omega) + 4\pi \nabla_\nu m_\nu(\vec{1}, \omega)|_{\vec{1} \to \vec{r}} = 0. \tag{23}$$

Thus, in consideration of the Landau–Lifshitz equations (21), (22), the dispersion relations of spin excitations are given by the eigenvalues of equation (23).

Let us consider the case when the temperature is low, and, therefore, diagrams containing blocks with isolated parts can be dropped. Since derivatives of the Brillouin function $B_S^{[n]}(p)$ in relation (5) tend to 0 exponentially with decreasing temperature, it follows that the contribution of these diagrams to effective propagators is negligible. Owing to this, from equation (22) we obtain that $m_z \to 0$, and equation (22) is dropped. In this case, in order to find the dispersion relations for spin excitations we should solve equations (21), (23). Equations (21)

are pseudodifferential equations and their solvability is determined by the existence of the parametrices $\hat{E}_{\pm}^{-1}$ of the Landau–Lifshitz operators $\hat{E}_{\pm}(\vec{r},\omega)$ [30]. Parametrices are inverse pseudodifferential operators modulo a pseudodifferential operator of order $-\infty$ and they can be determined by methods of the symbolic calculus. The parametrices $\hat{E}_{\pm}^{-1}$ exist on the functional space $\mathcal{F}$ orthogonal to the eigenvectors of operators $\hat{E}_{\pm}$ or to the kernel spaces $\mathrm{Ker}\hat{E}_{\pm} = \sum_j C_{\pm}^{j} m_{\pm}^{(0)j}(\vec{r},\omega)$, where $m_{\pm}^{(0)j}(\vec{r},\omega)$ are zero solutions of equations $\hat{E}_{\pm}(\vec{r},\omega)m_{\pm}^{(0)j}(\vec{r},\omega) = 0$. Discarding the zeroth eigensolutions $m_{\pm}^{(0)j}$ is equivalent to requiring that $m_{\pm}(\vec{1},\omega) = 0$ in relation (19) for zero values of the magnetic field $h_{\pm}(\vec{1},\omega)$, i.e. there does not exist a spin excitation with $m_{\pm}(\vec{1},\omega) \neq 0$ and $h_{\pm}(\vec{1},\omega) = 0$. Taking into account equation (21) and the condition that the parametrices $\hat{E}_{\pm}^{-1}$ exist on the space $\mathcal{F}$, from equation (23) we obtain the equation for the magnetostatic potential φ

$$\{\Delta + 8\pi[\nabla_{+}\hat{E}_{+}^{-1}(\vec{r},\omega)\gamma M(\vec{r})\nabla_{-} + \nabla_{-}\hat{E}_{-}^{-1}(\vec{r},\omega)\gamma M(\vec{r})\nabla_{+}]\}\varphi(\vec{r},\omega) = 0. \tag{24}$$

Equation (24) gives the dispersion relations of spin excitations and eigenfunctions $\varphi^{(\lambda)}(\vec{r},\omega)$ corresponding to effective propagators and interactions. The transition from the vector eigenfunctions $h_{\mu}^{(\lambda)}$ to the scalar eigenfunction $\varphi^{(\lambda)}$ leads to the simplification of relation (14): the indices $\mu_{j_1},\ldots,\mu_{j_\zeta}$ of the block factor $N^{(\bar{l})}_{\mu_{j_1}\ldots\mu_{j_\zeta}}$ and the corresponding summation can be dropped.

Consider a ferromagnetic film with the cubic lattice and with thickness $2d \gg a$. For a normal magnetized ($\vec{M} \parallel \mathrm{O}z$) homogeneous over thickness $z \in [-d,d]$ ferromagnetic film, the spectral parameter λ of eigenfunctions consists of the mode number j and the wavevector $\vec{q}$, and the eigensolutions of equation (24) are the wavefunctions [31]:

$$\varphi^{(j,\vec{q})}(x,y,z) = (2\pi)^{-1}\varphi^{(j)}(z)\exp(\mathrm{i}q_x x + \mathrm{i}q_y y)$$
$$\varphi^{(j)}(z) = f^{(j)-1/2}\begin{cases}\cos[q_z^{(j)}z + \pi(j-1)/2], & z \in [-d,d]\\ (-1)^{j-1}q_z^{(j)}\exp[q(d-z)]/q_0^{(j)}, & z \geqslant d\\ q_z^{(j)}\exp[q(d+z)]/q_0^{(j)}, & z \leqslant -d\end{cases} \tag{25}$$

where $j = 1,2,3,\ldots$ is the mode number, $q_0^{(j)2} = q^2 + q_z^{(j)2}$, $\vec{q}$ is the two-dimensional longitudinal wavevector, $q^2 = q_x^2 + q_y^2$, $f^{(j)} = d + q/q_0^{(j)2}$. The transverse wavevector $q_z^{(j)}$ is closely connected to the longitudinal wavevector $q = |\vec{q}|$ by the relation

$$2\cot 2q_z^{(j)}d = \frac{q_z^{(j)}}{q} - \frac{q}{q_z^{(j)}}. \tag{26}$$

For $q \ll q_z^{(j)}$, solutions of equation (26) are approximately equal to the expressions

$$j = 1: \qquad q_z^{(j)} = \sqrt{\frac{q}{d}} + \frac{q^{3/2}d^{1/2}}{2} + \mathrm{O}(q^2)$$
$$j > 1: \qquad q_z^{(j)} = \frac{\pi(j-1)}{2d} + \frac{2q}{\pi(j-1)} + \mathrm{O}(q^2).$$

The eigenfunctions $\varphi^{(j)}(z)$ form a set of complete orthogonal functions over the interval $[-d,d]$. The eigenvalues of equation (24) corresponding to $\varphi^{(j)}(z)$ determine the dispersion relations of spin waves

$$\omega^{(j)2}(\vec{q}) = \Omega^{(j)}(\Omega^{(j)} + \Omega_M q^2/q_0^{(j)2}), \tag{27}$$

where $\Omega^{(j)} = \gamma(H - 4\pi M + 4\pi\alpha M q_0^{(j)2})$, $\Omega_M = 4\pi\gamma M$, $q_0^{(j)}$ is the function of q given by equation (26). The derivation of the dispersion relation (27) with respect to q determines the group velocity of spin wave modes

$$v^{(j)}(\vec{q}) = \frac{\mathrm{d}\omega^{(j)}}{\mathrm{d}q} = \frac{\Omega_M[\alpha q_0^{(j)2}(1+qd)(2\Omega^{(j)}q_0^{(j)2} + \Omega_M q^2) + \Omega^{(j)}qq_z^{(j)2}d]}{\omega^{(j)}q_0^{(j)4}f^{(j)}}. \tag{28}$$

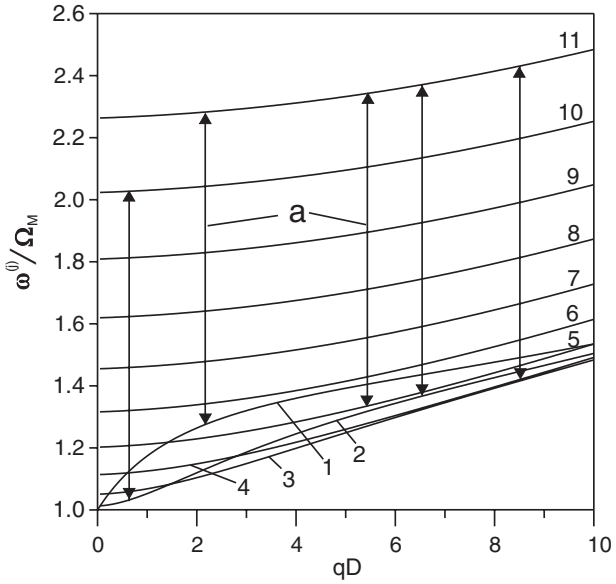

Figure 4. Dispersion curves for the first eleven FVMSW modes propagating in the YIG film of thickness $D = 0.5$ μm with $4\pi M = 1750$ Oe, $\alpha = 3.2 \times 10^{-12}$ cm^2 at the applied magnetic field $H = 3500$ Oe. a—Transitions between thermal excited spin wave modes with mode numbers i and k in the confluence process $\omega^{(j)}(0) + \omega^{(k)}(\vec{q}) = \omega^{(i)}(\vec{q})$ with the first ($j = 1$) long-wavelength spin wave mode. The confluence of the j-mode with the thermal excited k-mode forms the i-mode.

For $q \ll q_z^{(j)}$, the group velocity of the first mode is

$$v^{(1)}(\vec{q}) = \Omega_M \left(\frac{\alpha}{d} + \frac{d}{2} \right). \tag{29}$$

Spin waves with the magnetostatic potential (25) and the dispersion relations (27) propagating in normal magnetized films are called forward volume magnetostatic waves (FVMSWs) [5, 8, 9]. Dispersion curves for the first eleven FVMSW modes propagating in the YIG film of thickness $D = 2d = 0.5$ μm with $4\pi M = 1750$ Oe and $\alpha = 3.2 \times 10^{-12}$ cm^2 are shown in figure 4. The external magnetic field H is equal to 3500 Oe.

4.4. Dispersion relations and exchange boundary conditions

In the case when the sample size is much greater than the lattice constant, in the volume V of the ferromagnetic sample the pseudodifferential Landau–Lifshitz operators can be reduced to the differential operators

$$\hat{E}_{\pm}(\vec{r}, \omega) = \gamma[H(\vec{r}) + H^{(m)}(\vec{r}) - 4\pi\alpha M(\vec{r})\Delta] \pm \omega. \tag{30}$$

This reduction is not correct in the vicinity of the sample boundary ∂V. The linearized Landau–Lifshitz equations (21) with differential operators $\hat{E}_{\pm}(\vec{r}, \omega)$ given by relation (30) are used in [8, 9, 32–35]. For solvability of these equations the exchange boundary conditions are imposed:

$$\left. \frac{\partial m_\nu}{\partial \vec{n}} + \xi_i m_\nu \right|_{\partial V} = 0,$$

where $\vec{n}$ is the inward normal to the boundary ∂V, and ξ_i is the pinning parameter. For the case of a normal magnetized homogeneous film, the transverse wavevector $q_z^{(j)}$ is determined by the exchange boundary conditions and is given by the equation [8, 33]

$$\cot 2q_z^{(j)}d = \frac{q_z^{(j)2} - \xi_1\xi_2}{q_z^{(j)}(\xi_1 + \xi_2)}, \tag{31}$$

where ξ_1, ξ_2 are the pinning parameters on the upper and lower surfaces of the film.

The dispersion relations of spin waves are determined by solutions of equations (23) and (21) with the operators $\hat{E}_\pm(\vec{r}, \omega)$ (30) and with the exchange boundary conditions. The frequency of the j-mode is the function of $\vec{q}$, $q_z^{(j)}$ and is represented by the expression $\omega^{(j)2}(\vec{q}, q_z^{(j)}) = \Omega^{(j)}[\Omega^{(j)} + \Omega_M q^2/(q_z^{(j)2} + q^2)]$. The wavevector $q_z^{(j)}$ for spin waves with the exchange boundary conditions is given by equation (31). Making substitution of the solution of equation (31) for $q_z^{(j)}$ in the function $\omega^{(j)}(\vec{q}, q_z^{(j)})$, we obtain the dispersion relations $\omega^{(j)}(\vec{q})$, which are different from the dispersion relations (27). For $q \to 0$ the group velocity of the first mode tends to 0, in contrast with relation (29).

It should be noted that simultaneous solution of equations (23) and (21) with the operators $\hat{E}_\pm(\vec{r}, \omega)$ (30) and with the exchange boundary conditions is not reduced to the solutions of equations (21), (23) in the non-exchange approximation ($\alpha = 0$). In this approximation the transverse wavevector $q_z^{(j)}$ is determined by relation (26) [8]. By contrast, in the case of the exchange boundary conditions, $q_z^{(j)}$ is determined by relation (31) and does not tend to the solution of relation (26), when $\alpha \to 0$. This leads to different dispersion relations $\omega^{(j)}(\vec{q})$.

Moreover, in the case of the exchange boundary conditions, the inverse operators $\hat{E}_\pm^{-1}(\vec{r}, \omega)$ are determined on functional spaces, which are not orthogonal to the eigenvectors of operators $\hat{E}_\pm$ or to the kernel spaces $\mathrm{Ker}\,\hat{E}_\pm = \sum_j C_\pm^j m_\pm^{(0)j}(\vec{r}, \omega)$. The exchange boundary conditions lead to a finding of $C_\pm^j \neq 0$. This admits the existence of spin excitations only with a change in the magnetic moment $m_\pm$ for $h_\pm = 0$, that is in contradiction with relation (19). Summarizing, we conclude that the use of the exchange boundary conditions is incorrect.

4.5. $\mathcal{P}$-matrix for the case of normal magnetized ferromagnetic film

In order to find terms $Q^{(n,\mathrm{eff})}$ of the diagram expansion (14) for a normal magnetized film one needs to write the $\mathcal{P}$-matrix (10) in the representation of the functions $\varphi^{(j,\vec{q})}(\vec{r})$ given by relation (25). We consider the case when the absolute values of the wavevectors q, $q_z^{(j)}$, q', $q_z^{(j')}$ are much smaller than the reciprocal value of the lattice constant a^{-1} and, therefore, the substitution the integral for the sum $\sum_{\vec{1},\vec{1}'}$ in (13) is valid. Taking into account relations (10), (13), (15), explicit forms (2), (8) of the interaction and the matrix $\mathcal{G}^{(0)}$, we find that elements of the $\mathcal{P}$-matrix in the $\varphi^{(j,\vec{q})}(\vec{r})$-representation at low temperature are given by

$$\begin{aligned} P_{AB}(j, j', \vec{q}, \vec{q}', \omega_m) &= \int\int \varphi^{(j,\vec{q})*}(\vec{r}) P_{AB}(\vec{r}, \vec{r}', \omega_m) \varphi^{(j',\vec{q}')}\, \mathrm{d}^3r\, \mathrm{d}^3r' \\ &= F^{(j)} \bar{P}_{AB}(j, \vec{q}, \omega_m) \delta_{jj'} \delta(\vec{q} - \vec{q}'), \end{aligned} \tag{32}$$

where

$$\begin{aligned} &\bar{P}_{(1-)(1+)}(j, \vec{q}, \omega_m) = 2\rho V_a^2(\Omega^{(j)} + 2\eta_{-+}^{(j)} + \mathrm{i}\omega_m) \\ &\bar{P}_{(1+)(1+)}(j, \vec{q}, \omega_m) = -4\rho V_a^2 \eta_{--}^{(j)} \\ &\bar{P}_{(1-)(1-)}(j, \vec{q}, \omega_m) = -4\rho V_a^2 \eta_{++}^{(j)} \\ &\bar{P}_{(1z)(1\nu)}(j, \vec{q}, \omega_m) = \bar{P}_{(1\nu)(1z)}(j, \vec{q}, \omega_m) = \bar{P}_{(1z)(2\nu)}(j, \vec{q}, \omega_m) \\ &\qquad = \bar{P}_{(2\nu)(1z)}(j, \vec{q}, \omega_m) = 0 \qquad (\nu = -, +, z) \\ &\bar{P}_{(1-)(2-)}(j, \vec{q}, \omega_m) = \bar{P}_{(1+)(2+)}(j, \vec{q}, -\omega_m) \\ &\qquad = \left(\frac{B(p)}{\hbar}\tilde{I}(\vec{q}_0^{(j)}) - 2\eta_{-+}^{(j)}\right)(\Omega^{(j)} + \mathrm{i}\omega_m) + \frac{2B(p)}{\hbar}\tilde{I}(\vec{q}_0^{(j)})\eta_{-+}^{(j)} \end{aligned}$$

$$\bar{P}_{(1-)(2+)}(j,\vec{q},\omega_m) = -2\eta^{(j)}_{++}(\bar{p}+\mathrm{i}\omega_m)$$
$$\bar{P}_{(1+)(2-)}(j,\vec{q},\omega_m) = -2\eta^{(j)}_{--}(\bar{p}-\mathrm{i}\omega_m)$$
$$\bar{P}_{(1\pm)(2z)}(j,\vec{q},\omega_m) = -2\eta^{(j)}_{\mp z}(\Omega^{(j)}\mp\mathrm{i}\omega_m)$$
$$\bar{P}_{(2-)(2-)}(j,\vec{q},\omega_m) = -\rho^{-1}\eta^{(j)}_{--}(\bar{p}^2+\omega_m^2)$$
$$\bar{P}_{(2+)(2+)}(j,\vec{q},\omega_m) = -\rho^{-1}\eta^{(j)}_{++}(\bar{p}^2+\omega_m^2)$$
$$\bar{P}_{(2-)(2+)}(j,\vec{q},\omega_m) = \frac{1}{2}\rho^{-1}(\bar{p}+\mathrm{i}\omega_m)\left[\left(\frac{B(p)}{\hbar}\tilde{I}(\vec{q}_0^{(j)})-2\eta^{(j)}_{-+}\right)(\Omega^{(j)}-\mathrm{i}\omega_m)\right.$$
$$\left.+\frac{2B(p)}{\hbar}\tilde{I}(\vec{q}_0^{(j)})\eta^{(j)}_{-+}\right]$$
$$\bar{P}_{(2\pm)(2z)}(j,\vec{q},\omega_m) = -\rho^{-1}\eta^{(j)}_{\pm z}(\bar{p}\mp\mathrm{i}\omega_m)(\Omega^{(j)}\pm\mathrm{i}\omega_m)$$
$$\bar{P}_{(2z)(2z)}(j,\vec{q},\omega_m) = F^{(j)-1}\beta V_a I(\vec{q}_0^{(j)}) - \rho^{-1}\eta^{(j)}_{zz}(\Omega^{(j)2}+\mathrm{i}\omega_m^2)$$
$$F^{(j)} = (\omega^{(j)2}+\omega_m^2)^{-1}, \qquad \rho = \frac{B(p)}{\beta\hbar V_a}, \qquad \bar{p} = \gamma H_z^{(c)}$$
$$\eta^{(j)}_{\mu\nu} = \frac{\Omega_M q_\mu q_\nu}{q_0^{(j)2}} \qquad (\mu,\nu = -,+,z)$$
$$q_\pm = \tfrac{1}{2}(q_x \mp \mathrm{i}q_y), \qquad \tilde{I}(\vec{q}_0^{(j)}) = \tilde{I}(0) - wq_0^{(j)2}.$$

Besides this, the symmetry relation $\bar{P}_{(a\mu)(b\nu)}(j,\vec{q},\omega_m) = \bar{P}_{(b\nu)(a\mu)}(j,\vec{q},-\omega_m)$ holds.

In the representation of the functions (25) the block factor $N^{(\bar{l})}$ in the terms $Q^{(n,\mathrm{eff})}$ (14) of the diagram expansion is written as

$$N^{(\bar{l})}(j_1,\vec{q}_1,\omega_{m_1};\ldots;j_\zeta,\vec{q}_\zeta,\omega_{m_\zeta}) = \bar{N}^{(\bar{l})}(j_1,\vec{q}_1;\ldots;j_\zeta,\vec{q}_\zeta)\delta\left(\sum_{k=1}^{\zeta}\vec{q}_k\right)$$
$$= \frac{1}{2(4\pi)^{\zeta-2}V_a}\prod_{k=1}^{\zeta} f^{(j_k)-1/2}\sum_{\sigma_1,\ldots,\sigma_\zeta}\frac{\sin\left(\sum_{k=1}^{\zeta}\sigma_k q_z^{(j_k)}\right)d}{\sum_{k=1}^{\zeta}\sigma_k q_z^{(j_k)}}$$
$$\times\ \exp\left(\mathrm{i}\sum_{k=1}^{\zeta}\sigma_k\pi(j_k-1)/2\right)\delta\left(\sum_{k=1}^{\zeta}\vec{q}_k\right), \tag{33}$$

where $\bar{l}$ is the block in the *Eff*-diagram, in which ζ lines come in; $\sigma_k = \pm 1$; $\sum_{\sigma_1,\ldots,\sigma_\zeta}$ denotes the summation over all sets $\{\sigma_1,\ldots,\sigma_\zeta\}$.

In the case of ferromagnetic films the summation over a set of spectral parameters $\{\lambda_1,\ldots,\lambda_n\}$ for terms $Q^{(n,\mathrm{eff})}$ in (14) of the diagram expansion is transformed to the summation over mode numbers $\{j_1,\ldots,j_n\}$ and the integration over longitudinal wavevectors $\{\vec{q}_1,\ldots,\vec{q}_n\}$:

$$\sum_{\lambda_1,\ldots,\lambda_n} \longrightarrow \int\ldots\int \mathrm{d}^2q_1\ldots\mathrm{d}^2q_n\sum_{j_1,\ldots,j_n}.$$

It follows from relation (33) that the sum of longitudinal wavevectors, which come in and go out from a block, is conserved: $\sum_{k=1}^{\zeta}\vec{q}_k = 0$. The conservation law for transverse wavevectors $\sum_{k=1}^{\zeta}\sigma_k q_z^{(j_k)}$ in a block takes place only when $d\to\infty$.

5. Relaxation of spin wave modes

Consider a three-spin-wave confluence process. We will obtain an explicit expression describing relaxation of spin waves (FVMSWs) in the normal magnetized homogeneous ferromagnetic film, when the following assumptions are satisfied simultaneously:
1. *Low-temperature approximation.* Since derivatives of the Brillouin function $B_S^{[n]}(p)$ tend to 0 exponentially with decreasing temperature, it follows that diagrams containing blocks with isolated parts can be dropped [18].
2. *One-loop approximation.* Because every sum over $\vec{q}$, $q_z^{(j)}$ is proportional to $V_a/R_{\rm int}^3$, where $R_{\rm int}$ is the radius of the interaction between spins, then the diagrams containing n loops give correction terms to the Green functions $G_{\mu\nu}$ in equation (15) and to the $\mathcal{P}$-matrix in relation (10) proportional to $(V_a/R_{\rm int}^3)^n$ [18, 19]. For $V_a/R_{\rm int}^3 \ll 1$ the one-loop diagrams give the greatest correction term to $G_{\mu\nu}$ and to $\mathcal{P}$. If the MDI is taken into account, then the one-loop diagrams are different from zero. The one-loop diagrams correspond with the three-magnon processes induced by the MDI. The exchange interaction cannot induce three-magnon processes. Therefore, if the MDI is discarded, it determines non-trivial diagrams only in the two-loop approximation.
3. *Approximation of small longitudinal wavevectors: $q \ll q_z^{(j)}$.* We consider a relaxation of long-wavelength spin waves, when the absolute value of the wavevector $q_0^{(j)}$ is much smaller than the reciprocal value of the lattice constant a^{-1}. Therefore, the substitution of the integral for the sum over lattice sites is valid.

The correction terms to the spin wave spectrum and the relaxation are determined by self-energy diagram insertions to the $\mathcal{P}$-matrix given by relation (32). These diagrams cannot be divided into two parts through breaking a line. Analytical expressions of the self-energy diagrams form the self-energy matrix $\hat{\Sigma} = \|\Sigma_{AB}\|$. Damping of excitations is defined by the imaginary part of the pole of the forming matrix $\mathcal{P}^{(\Sigma)} = \|P_{AB}^{(\Sigma)}\|$ with insertions under the analytical continuation (11). The matrix $\mathcal{P}^{(\Sigma)}$ is connected with the $\mathcal{P}$-matrix by the equation of the Dyson type

$$\begin{aligned} P_{AB}^{(\Sigma)}(j, j', \vec{q}, \vec{q}', \omega_m) &= P_{AB}(j, j', \vec{q}, \vec{q}', \omega_m) \\ &+ \frac{1}{V_a^2} \sum_{j_1, j_2, C, D} \int\int P_{AC}^{(\Sigma)}(j, j_1, \vec{q}, \vec{q}_1, \omega_m) \Sigma_{CD}(j_1, j_2, \vec{q}_1, \vec{q}_2, \omega_m) \\ &\times P_{DB}(j_2, j', \vec{q}_2, \vec{q}', \omega_m)\, \mathrm{d}^2\vec{q}_1\, \mathrm{d}^2\vec{q}_2. \end{aligned} \tag{34}$$

The factor V_a^{-2} in equation (34) appears due to the transition from the lattice variables $\vec{1}$ to the spatial variables $\vec{r}$. Taking into account the explicit form (32) of the $\mathcal{P}$-matrix for normal magnetized films, we obtain that in the approximation $q \ll q_z^{(j)}$ the $\mathcal{P}$-matrix can be written as

$$\mathcal{P} = \begin{pmatrix} 0 & P_{(1-)(1+)} & 0 & \vdots & P_{(1-)(2-)} & 0 & 0 \\ P_{(1+)(1-)} & 0 & 0 & \vdots & 0 & P_{(1+)(2+)} & 0 \\ 0 & 0 & 0 & \vdots & 0 & 0 & 0 \\ \cdots & \cdots & \cdots & \cdots & \cdots & \cdots & \cdots \\ P_{(2-)(1-)} & 0 & 0 & \vdots & 0 & P_{(2-)(2+)} & 0 \\ 0 & P_{(2+)(1+)} & 0 & \vdots & P_{(2+)(2-)} & 0 & 0 \\ 0 & 0 & 0 & \vdots & 0 & 0 & P_{(2z)(2z)} \end{pmatrix}. \tag{35}$$

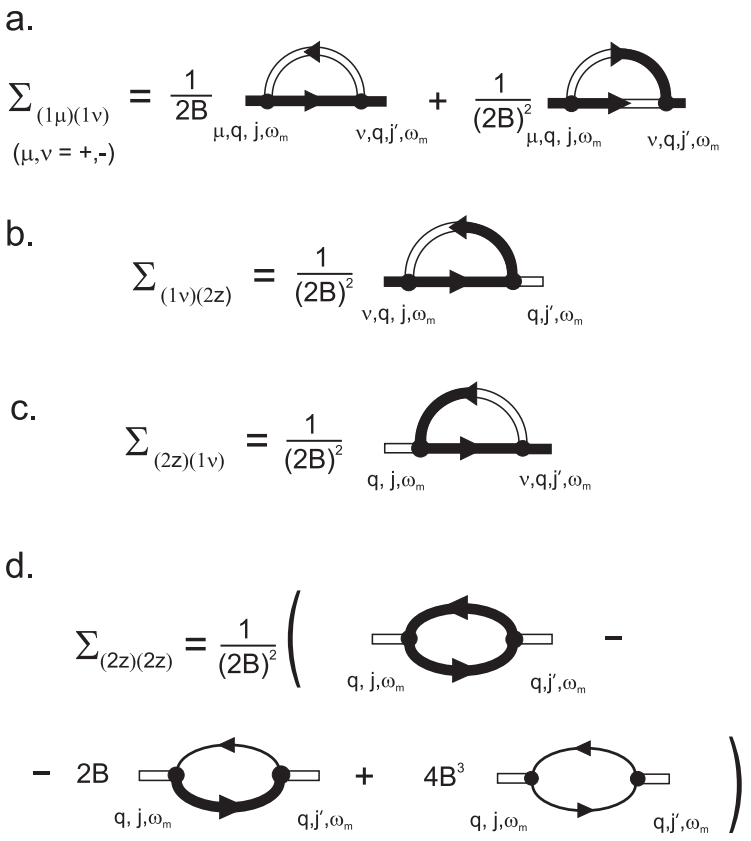

Figure 5. Self-energy diagrams Σ_{AB} in the low-temperature one-loop approximation. Second and third diagrams in (d) are needed to perform partial summation and substitution of effective propagators for bare propagators in the first diagram. The coefficients before diagrams are ξ-factors in the diagram expansion (14).

The low-temperature and one-loop approximations define the self-energy matrix $\hat{\Sigma}$:

$$\hat{\Sigma} = \begin{pmatrix} \Sigma_{(1-)(1-)} & \Sigma_{(1-)(1+)} & 0 & \vdots & 0 & 0 & \Sigma_{(1-)(2z)} \\ \Sigma_{(1+)(1-)} & \Sigma_{(1+)(1+)} & 0 & \vdots & 0 & 0 & \Sigma_{(1+)(2z)} \\ 0 & 0 & 0 & \vdots & 0 & 0 & 0 \\ \cdots & \cdots & \cdots & \cdots & \cdots & \cdots & \cdots \\ 0 & 0 & 0 & \vdots & 0 & 0 & 0 \\ 0 & 0 & 0 & \vdots & 0 & 0 & 0 \\ \Sigma_{(2z)(1-)} & \Sigma_{(2z)(1+)} & 0 & \vdots & 0 & 0 & \Sigma_{(2z)(2z)} \end{pmatrix}. \tag{36}$$

Each non-zero element of the $\hat{\Sigma}$-matrix is described by a one-loop diagram with two e-vertices (figure 5). If we consider the spin wave mode j in the frequency range where its dispersion curve does not intersect with dispersion curves of other modes, then from equation (34) we find that the pole of the matrix $\mathcal{P}^{(\Sigma)}$ is determined by the equation

$$\det\left[1 - \sum_D \bar{\Sigma}_{CD}(j, j, \vec{q}, \omega_m) F^{(j)} \bar{P}_{DB}(j, \vec{q}, \omega_m)\right]\Big|_{i\omega_m \to \omega + i\varepsilon\,\mathrm{sgn}\,\omega} = 0, \tag{37}$$

where the regular part $\bar{\Sigma}_{CD}$ is connected with Σ_{CD} by the relation $\Sigma_{CD}(j, j', \vec{q}, \vec{q'}, \omega_m) = \bar{\Sigma}_{CD}(j, j', \vec{q}, \omega_m)V_a\delta(\vec{q} - \vec{q'})$. $F^{(j)}$ and $\bar{P}_{DB}$ are defined in relations (32).

Taking into account the forms of $\mathcal{P}$- and $\hat{\Sigma}$-matrices (35), (36), we perform the polynomial decomposition of the determinant (37) with respect to $\bar{\Sigma}_{CD}$. Then, neglecting higher orders and holding linear terms containing $\bar{\Sigma}_{CD}$ in the decomposition, we obtain that the term with $\bar{\Sigma}_{(1+)(1-)}$, which is determined by two diagrams in figure 5(a), makes a major contribution to the pole singularity of the $\mathcal{P}^{(\Sigma)}$-matrix. In this case, equation (37) is simplified:

$$1 - \bar{\Sigma}_{(1+)(1-)}(j, j, \vec{q}, \omega_m)F^{(j)}\bar{P}_{(1-)(1+)}(j, \vec{q}, \omega_m)]|_{i\omega_m \to \omega + i\varepsilon\,\mathrm{sgn}\,\omega} = 0.$$

Substituting $F^{(j)}$, $\bar{P}_{(1-)(1+)}$ according to relations (32), we find the relationship between the reciprocal lifetime of spin waves $\delta\omega^{(j)}$ and the imaginary part $\bar{\Sigma}_{(1+)(1-)}$:

$$\delta\omega^{(j)}(\vec{q}) = \frac{2B(p)V_a}{\hbar\beta}\,\mathrm{Im}\,\bar{\Sigma}_{(1+)(1-)}(j, j, \vec{q}, \omega_m)|_{i\omega_m \to \omega + i\varepsilon\,\mathrm{sgn}\,\omega}.$$

The analytical expressions for diagrams of the self-energy matrix element $\bar{\Sigma}_{(1+)(1-)}$ are determined by rules of the diagram technique for analytical expressions (14) of the *Eff*-diagrams:

$$\begin{aligned}\bar{\Sigma}_{(1+)(1-)}(j, j, \vec{q}, \omega_m) = {} & \frac{1}{4B(p)}\sum_{n,i,k} \\ & \times \int F^{(i)}F^{(k)}[\bar{P}_{(1-)(1+)}(i, -\vec{q}_1, -\omega_n)\bar{P}_{(2z)(2z)}(k, \vec{q} - \vec{q}_1, \omega_m - \omega_n) \\ & + \frac{1}{8B(p)}\bar{P}_{(1-)(2z)}(i, \vec{q}_1, \omega_n)\bar{P}_{(2z)(1+)}(k, \vec{q} - \vec{q}_1, \omega_m - \omega_n)] \\ & \times \bar{N}^2(j, \vec{q}; i, \vec{q}_1; k, \vec{q} - \vec{q}_1)\,\mathrm{d}^2q_1,\end{aligned}$$

where the block factor $\bar{N}$ is given by relation (33).

Summing over the frequency variable ω_n and performing the analytical continuation, for $\beta\hbar\omega^{(p)} \ll 1 (p = j, i, k)$ we get the final expression of the damping for the spin wave mode j:

$$\begin{aligned}\Delta^{(j)}(\vec{q}) = \frac{\delta\omega^{(j)}(\vec{q})}{\omega^{(j)}} = {} & \frac{V_a}{16\pi\beta\hbar f^{(j)}}\sum_{i,k,s}\int \frac{\Xi^2_{jik}}{f^{(i)}f^{(k)}\omega^{(i)2}\omega^{(k)2}|v^{(i)} - v^{(k)}|} \\ & \times \left[\left(\Omega^{(i)} + 2\eta^{(i)}_{-+} + \omega^{(i)}\right)\Omega^{(k)}\eta^{(k)}_{zz}\eta^{(k)}_{-+} + \left(\Omega^{(k)} + 2\eta^{(k)}_{-+} - \omega^{(k)}\right)\Omega^{(i)}\eta^{(i)}_{zz}\eta^{(i)}_{-+}\right. \\ & \left. + \frac{1}{16B(p)}\left(\Omega^{(i)} + \omega^{(i)}\right)\left(\Omega^{(k)} - \omega^{(k)}\right)\left(\eta^{(i)}_{+z}\eta^{(k)}_{-z} + \eta^{(i)}_{-z}\eta^{(k)}_{+z}\right)\right]\delta(\vec{q}_1 - \vec{q}^{(s)})\,\mathrm{d}^2q_1,\end{aligned} \tag{38}$$

where $\vec{q}^{(s)}$ is the solution of the equation

$$\omega^{(j)}(\vec{q}) = \omega^{(i)}(\vec{q}^{(s)}) - \omega^{(k)}(\vec{q} - \vec{q}^{(s)}); \tag{39}$$

$$\Xi_{jik} = \sum_{\sigma_i,\sigma_k=\pm1}\frac{\sin(q_z^{(j)} + \sigma_i q_z^{(i)} + \sigma_k q_z^{(k)})d}{q_z^{(j)} + \sigma_i q_z^{(i)} + \sigma_k q_z^{(k)}}\cos[\pi(j + \sigma_i i + \sigma_k k - 3)/2];$$

$v^{(i)} = v^{(i)}(\vec{q}_1)$, $v^{(k)} = v^{(k)}(\vec{q} - \vec{q}_1)$ are the group velocities of i- and k-modes given by equation (28) at the wavevectors $\vec{q}_1$ and $\vec{q} - \vec{q}_1$, respectively. Values of $q_z^{(i)}$, $q_0^{(i)}$, $\omega^{(i)}$, $\Omega^{(i)}$, $\eta^{(i)}_{\mu\nu}$, $f^{(i)}$ are calculated at the wavevector $\vec{q}_1$, and values of $q_z^{(k)}$, $q_0^{(k)}$, $\omega^{(k)}$, $\Omega^{(k)}$, $\eta^{(k)}_{\mu\nu}$, $f^{(k)}$ are calculated at the vector $\vec{q} - \vec{q}_1$.

Relation (38) describes relaxation of the long-wavelength spin wave j-mode caused by inelastic scattering on thermally excited spin wave modes. Relaxation occurs through the

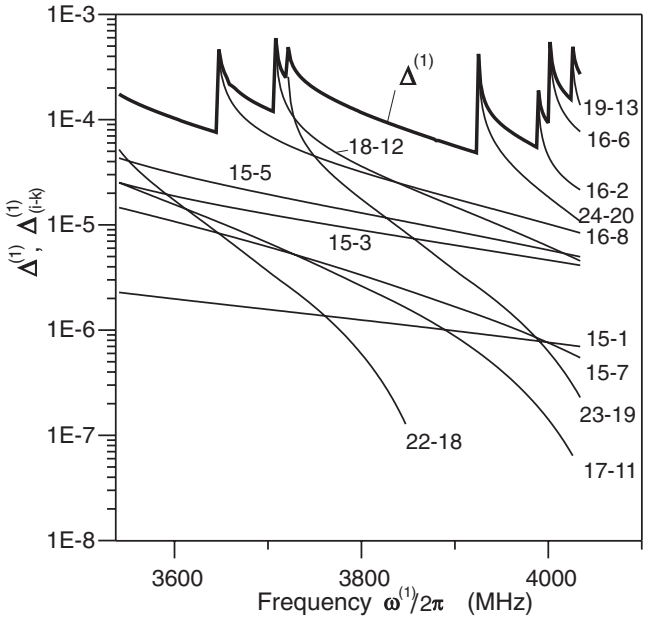

Figure 6. Damping $\Delta^{(1)} = \sum_{i,k} \Delta^{(1)}_{(i,k)}$ and partial dampings $\Delta^{(1)}_{(i,k)}$ for the first spin wave mode (FVMSW) propagating in a YIG film with thickness $D = 0.8$ μm, $4\pi M = 1750$ Oe, $\alpha = 3.2 \times 10^{-12}$ cm^2 at $H = 3000$ Oe, $T = 300$ K. Partial dampings $\Delta^{(1)}_{(i,k)}$ are determined by transitions i–k between i- and k-modes.

confluence of the j-mode with the k-mode to form the i-mode. The confluence processes are induced by the MDI and are accompanied by transitions between thermally excited i- and k-modes (figure 4). Numerical calculation gives that the confluence processes with thermally excited spin wave modes with small indices are most efficient. From the explicit form of Ξ_{jik} it follows that confluence processes take place when the sum of mode numbers $j + i + k$ is equal to an odd number. The three-spin-wave confluence processes induced by the MDI are the dominant relaxation mechanism in pure YIG, $Li_{0.5}Fe_{2.5}O_4$, $CdCr_2Se_4$, and EuO [7–14]. The damping $\Delta^{(j)}$ increases directly proportionally to the temperature. The linear temperature dependence of $\Delta^{(j)}$ is characteristic for all three-spin-wave confluence processes independently of the shape sample. This is in accordance with the linear temperature dependence of ΔH in YIG and $Li_{0.5}Fe_{2.5}O_4$ observed in [10, 12].

From equation (38) it follows that the damping can be regarded as the sum of partial dampings: $\Delta^{(j)} = \sum_{i,k} \Delta^{(j)}_{(i,k)}$. The partial damping $\Delta^{(j)}_{(i,k)}$ is determined by transitions $i - k$ between i- and k-modes. Transitions take place when equation (39) has at least one solution $\vec{q}^{(s)}$ for the given $\vec{q}$. Figure 6 shows frequency dependences of the damping $\Delta^{(1)}$ and partial dampings $\Delta^{(1)}_{(i,k)}$, which make a major contribution to $\Delta^{(1)}$. Calculations have been done for a YIG film with thickness $D = 0.8$ μm at $H = 3000$ Oe. It can be seen that the peaks in the frequency dependence of $\Delta^{(1)}$ originate from extreme points of partial dampings. For example, for the transition 16–8 ($i = 16$, $k = 8$) the frequency $\omega^{(1)}/2\pi$ in the range (3537.5–3647.4 MHz) is less than $(\omega^{(i)}(\vec{q}^{(s)}) - \omega^{(k)}(\vec{q} - \vec{q}^{(s)}))/2\pi$ for any $\vec{q}^{(s)}$, equation (39) has no solution, and the transition is not induced. At the frequency $\omega^{(1)}/2\pi = 3647.4$ MHz equation (39) has the single solution $|\vec{q}^{(s)}| = 29.66/D$ and the transition 16–8 begins to make a contribution to $\Delta^{(1)}$. At frequencies $\omega^{(1)}/2\pi > 3647.4$ MHz equation (39) has two solutions and there are two transitions between modes with numbers 16 and 8.

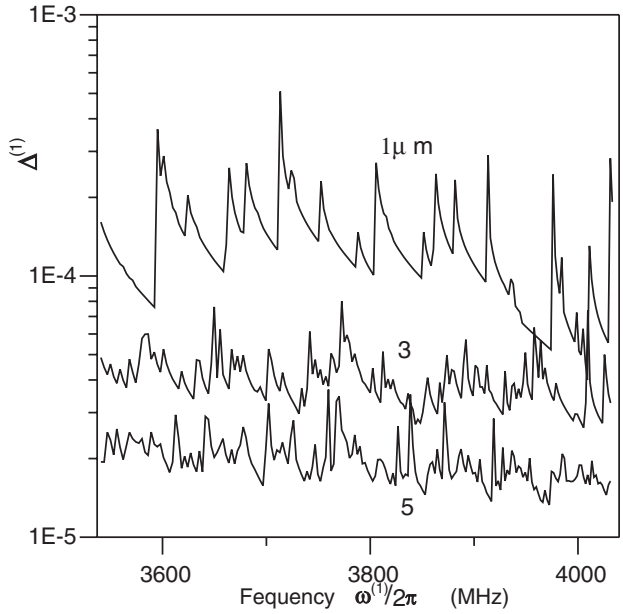

Figure 7. Damping $\Delta^{(1)}$ for the first spin wave mode (FVMSW) propagating in a YIG film with $4\pi M = 1750$ Oe, $\alpha = 3.2 \times 10^{-12}$ cm^2 at $H = 3000$ Oe, $T = 300$ K for different thickness D (1, 3, and 5 μm).

Let us analyse changes of the damping (38) upon changing the film thickness, the applied magnetic field H, and the mode number j. Calculations are performed for YIG films with $4\pi M = 1750$ Oe, $\alpha = 3.2 \times 10^{-12}$ cm^2 at the temperature $T = 300$ K. We take into account 120 thermally excited spin wave modes in the confluence processes.

1. Spin wave damping versus film thickness

Calculations are carried out for the first spin wave mode ($j = 1$) propagating in a YIG film. The film is normal magnetized by the magnetic field $H = 3000$ Oe. We investigate the frequency dependences of the damping $\Delta^{(1)}$ for different values of the thickness D. The damping decreases with increasing film thickness (figure 7). For $D \to \infty$ the damping $\Delta^{(1)}$ tends to 0. With increasing film thickness D, the density of dispersion curves of modes on the plane (ω, q) increases and the frequency of the spacings between curves decreases. This leads to an increase of the density of peaks on the frequency dependence of the damping for greater values of D. Simultaneously, for thick films peak heights decrease and the frequency dependences of the damping is smoothed. In the next experiment we plan to verify the peak character of the damping in thin films predicted by the developed theory.

2. Spin wave damping versus applied magnetic field

Figure 8 shows the damping $\Delta^{(1)}$ of the first spin wave mode versus the longitudinal wavevector q normalized by the film thickness D. In this case, the dependence of the damping versus q is more convenient than the frequency dependence, because, according to equation (27), the frequency $\omega^{(j)}$ depends on the magnetic field H and, therefore, domains of definition of frequency dependences are different for different magnetic fields. At the same time, domains of definition of dependences of the damping versus q coincide. The frequency $\omega^{(j)}$ can be

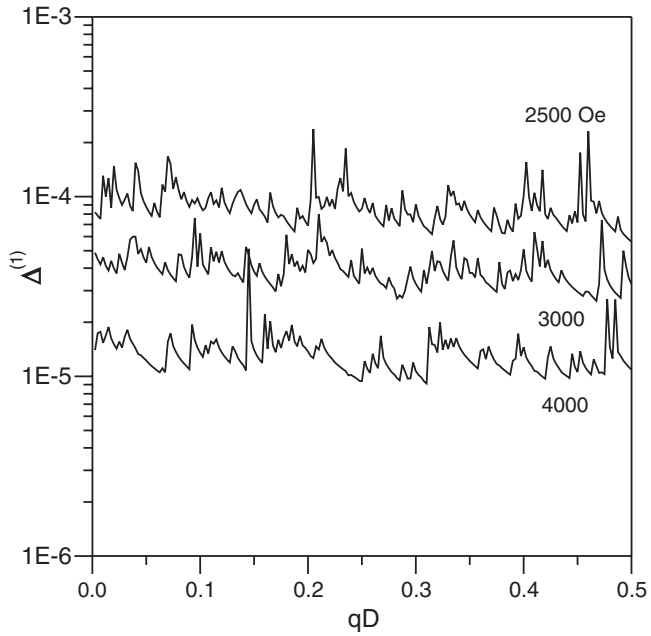

Figure 8. Damping $\Delta^{(1)}$ for the first spin wave mode (FVMSW) propagating in a YIG film of thickness 3 μm with $4\pi M = 1750$ Oe, $\alpha = 3.2 \times 10^{-12}$ cm^2 at $T = 300$ K for different values of the applied magnetic field H (2500, 3000, and 4000 Oe).

easily expressed via q. At the given H for the given j-mode $\omega^{(j)}$ is the single-valued function of the wavevector q. Dependences are calculated for the thickness $D = 3$ μm at different magnetic fields H. The damping $\Delta^{(1)}$ decreases with increasing applied magnetic field H.

3. Spin wave damping versus the mode number

Calculations are carried out for a YIG film of thickness $D = 3$ μm at the applied magnetic field $H = 3000$ Oe (figure 9). It is found that, on average, for the first mode the value of $\Delta^{(1)}$ is less than values of $\Delta^{(j)}$ for modes with the number $j \geqslant 2$. This can be accounted for by different overlapping of wavefunctions (25) of three modes in the confluence processes.

Relation (38) for the damping, which is determined by the confluence processes induced by the MDI, gives values which correspond to experimental ones. For homogeneous YIG films, experimental values of the damping $\Delta^{(j)}$ are, usually, 10^{-4} at $T = 300$ K [8, 9]. This value corresponds to the values of $\Delta^{(j)}$ presented in figures 6–9 with respect to the order of magnitude. If MDI is discarded, the damping is determined by the exchange interaction in the two-loop approximation and is much lower. Using relations given in [18], we have found that in this case for the YIG film with $D = 3$ μm, $qD = 0.25$ at $H = 3000$ Oe the two-loop diagrams with the exchange interaction give the damping $\Delta^{(1)}$ equal to 10^{-7}.

It is necessary to notice that the q_z-wavevector conservation condition for damping (38) is not satisfied. This leads to the effective relaxation of the uniform precession induced by the three-magnon processes. Previous studies of the spin wave damping at small wavevectors were carried out for infinite or semi-infinite ferromagnets [11, 15–17]. For these ferromagnets both energy and wavevector conservation conditions are satisfied and the three-magnon processes do not contribute to the line width in a usual resonant experiment. This discrepancy between

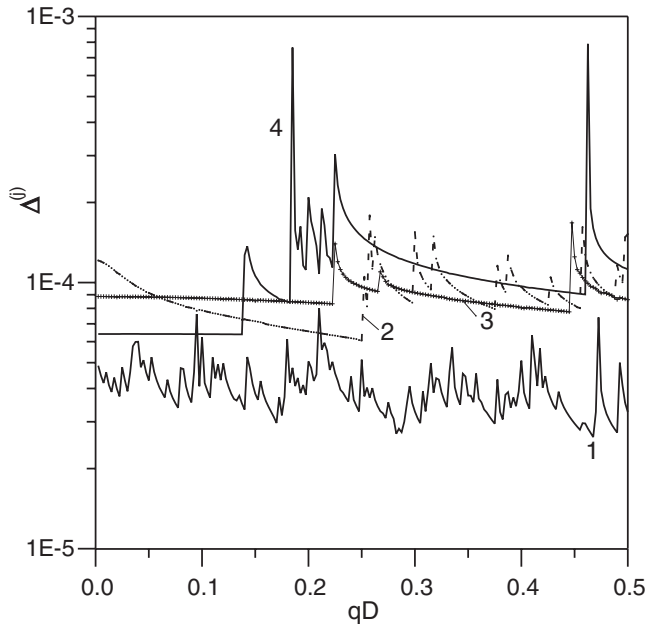

Figure 9. Damping $\Delta^{(j)}$ for spin wave modes (FVMSWs) with different mode numbers j propagating in a YIG film of thickness $D = 3$ μm with $4\pi M = 1750$ Oe, $\alpha = 3.2 \times 10^{-12}$ cm^2 at $H = 3000$ Oe, $T = 300$ K. $j = 1$–4.

theoretical and experiment results is removed in the framework of the developed model of the spin wave relaxation in finite ferromagnetic samples, where the wavevector conservation conditions are not held. It is worth mentioning that, by analogy with the damping in infinite ferromagnets, a sharp decrease of the three-magnon damping at small in-plane wavevectors for EuO films and Fe films was obtained in the framework of the microscopic theory of the dipole–exchange spin waves for ultrathin films in [23]. In all probability, this decrease is caused by the fact that the MDI has not been renormalized. By contrast, in our work we renormalize both Green functions and interactions as $\mathcal{P}$-matrix elements, and find the effective propagators and interactions, and this decrease of the damping is removed.

6. Conclusion

We have investigated spin excitations and relaxation of spin wave modes in the Heisenberg model with the dipole–exchange interaction by the spin operator diagram technique and have obtained the following results.

(1) Generalized Landau–Lifshitz equations, which are derived from first principles, have the pseudodifferential form. Spin excitations (spin wave modes) are determined by simultaneous solution of the Landau–Lifshitz equations and the equation for the magnetostatic potential. Eigenvalues of the equation for the magnetostatic potential give the spin wave spectrum. Due to the long-range character, the relatively weak magnetic dipole interaction (MDI) transforms the spin wave spectrum to the spectrum of the discrete mode type depending on the dimensions and shapes of the ferromagnetic samples. The use of exchange boundary conditions for solvability of the Landau–Lifshitz equations is incorrect.

(2) In the framework of the considered Heisenberg model with the dipole–exchange interaction, the MDI makes a major contribution to the relaxation of long-wavelength spin waves and the uniform precession in comparison with the exchange interaction. Due to the MDI, the damping is determined by diagrams in the one-loop approximation, which correspond to the confluence of two spin waves. The exchange interaction gives non-trivial terms in the damping only in the two-loop approximation, and these terms are small. We have calculated the damping induced by the MDI at low temperatures for a normal magnetized ferromagnetic film. It is obtained that the relaxation of the long-wavelength spin wave j-mode occurs through the confluence of the j-mode with the thermally excited k-mode to form the i-mode. The confluence process takes place when the sum of mode indices $j + i + k$ is equal to an odd number. The damping decreases with increasing film thickness and applied magnetic field and increases directly proportionally to the temperature. For modes with high mode numbers the spin wave damping is higher than for the first spin wave mode. The developed theory predicts the peak character of the damping in thin films. The considered three-spin-wave confluence processes induced by the MDI are the dominant relaxation mechanism in pure YIG, $Li_{0.5}Fe_{2.5}O_4$, $CdCr_2Se_4$, and EuO. The results of this work are applicable to microwave spin wave devices, new tunnelling microscopy based on the time-resolved Kerr effect and devices based on localized spin wave modes in nanosized magnetic dots and wires.

Acknowledgment

This work was supported by the Russian Foundation for Basic Research, grant no 04-02-16599.

References

[1] Gubbiotti G, Conti M, Carlotti G, Candeloro P, Di Fabrizio E, Guslienko K Yu, Andre A, Bayer C and Slavin A N 2004 *J. Phys.: Condens. Matter* **16** 7709
[2] Park J P, Eams P, Engebretson D M, Berezovsky J and Crowell P A 2002 *Phys. Rev. Lett.* **89** 277201
[3] Bayer C, Park P, Wang H, Yan M, Campbell C E and Crowell P A 2004 *Phys. Rev.* B **69** 134401
[4] Tamaru S, Bain J A, van der Veerdonk R J M, Crawford T M, Covington M and Kryder M H 2004 *Phys. Rev.* B **70** 104416
[5] Stancil D D 1993 *Theory of Magnetostatic Waves* (New York: Springer)
[6] Kabos P and Stalmachov V S 1994 *Magnetostatic Waves and Their Applications* (New York: Chapman and Hall)
[7] Krupička S 1973 *Physik der Ferrite und der Verwandten Magnetischen Oxide* (Prag: Academia Verlag der Tschechoslowakischen)
[8] Gurevich A G and Melkov G A 1996 *Magnetization Oscillations and Waves* (New York: CRC Press)
[9] Gurevich A G 1973 *Magnetic Resonance in Ferrites and Antiferromagnetics* (Moscow: Nauka)
[10] Le Craw R C and Spencer E G 1962 *J. Phys. Soc. Japan* **17** (Suppl. B1) 401
[11] Kolokolov I V, L'vov V S and Cherepanov V B 1984 *Sov. Phys.—JETP* **59** 1131
[12] Yakovlev Yu M, Rubal'skaya E V, Godes L G, Lapovok B L and Bushueva T N 1971 *Sov. Phys.—Solid State* **13** 1151
[13] Anisimov A N, Shukyurov A S, Gurevich A G and Emiryan L M 1983 *Sov. Phys.—JETP* **57** 818
[14] Gurevich A G, Anisimov A N, Samokhvalov A A and Solin N I 1985 *Acta Phys. Pol.* A **68** 467
[15] Sparks M 1964 *Ferromagnetic Relaxation Theory* (New York: Mc Graw-Hill)
[16] Sparks M, Loudon R and Kittel C 1961 *Phys. Rev.* **122** 791
[17] Schlömann E 1961 *Phys. Rev.* **121** 1312
[18] Izyumov Yu A, Kassan-ogly F A and Skryabin Yu N 1974 *Field Methods in the Theory of Ferromagnetism* (Moscow: Nauka)
[19] Vaks V G, Larkin A I and Pikin S A 1967 *Sov. Phys.—JETP* **53** 281
[20] Vaks V G, Larkin A I and Pikin S A 1967 *Sov. Phys.—JETP* **53** 1089
[21] White R W 1983 *Quantum Theory of Magnetism* (Berlin: Springer)

[22] Abrikosov A A, Gor'kov L P and Dzyaloshinski I E 1975 *Methods of Quantum Field Theory in Statistical Physics* (New York: Dover)
[23] Costa Filho R N, Cottam M G and Farias G A 2000 *Phys. Rev.* B **62** 6545
[24] Matsubara T 1955 *Prog. Theor. Phys.* **14** 351
[25] Vasil'ev A N 1997 *Functional Methods in Quantum Field Theory and Statistical Physics* (New York: Taylor and Francis)
[26] Vedmedenko E Y, Oepen H P and Kirschner J 2003 *Phys. Rev.* B **67** 012409
[27] Vedmedenko E Y, Oepen H P and Kirschner J 2003 *Phys. Rev. Lett.* **90** 137203
[28] Akhiezer A I, Bar'yakhtar V G and Peletminskii S V 1968 *Spin Waves* (Amsterdam: North-Holland)
[29] Zubarev D N 1974 *Nonequilibrium Statistical Thermodynamics* (New York: Plenum)
[30] Treves F 1982 *Introduction to Pseudodifferential and Fourier Integral Operators* vol 1 (New York: Plenum)
[31] Lutsev L V 1995 *J. Techn. Phys.* **40** 139
[32] Soohoo R F 1965 *Magnetic Thin Films* (New York: Harper and Row)
[33] Kalinikos B A and Slavin A N 1986 *J. Phys. C: Solid State Phys.* **19** 7013
[34] Kalinikos B A, Kozhus N V, Kostylev M P and Slavin A N 1990 *J. Phys.: Condens. Matter* **2** 9861
[35] Zyuzin A M, Sabaev S N and Kulyapin A V 2003 *Phys. Solid State* **45** 2313